JOURNAL OF MATERIALS SCIENCE 26 (1991) 5733–5740

Fractographic examinations of fracture in polycrystalline S2 ice

YINGCHANG WEI, J. P. DEMPSEY
Department of Civil and Environmental Engineering, Clarkson University, Potsdam, NY 13699-5710, USA

Fractographic examinations were carried out on the fracture surfaces of both single-edge notched bend (SENB) and wedge-loaded compact tension (WLCT) specimens of S2 freshwater ice. Formvar solutions provided an effective means of making replicas that revealed various patterns of the fracture surfaces. The fracture modes consisted of both cleavage and brittle intergranular fracture, with cleavage fracture dominating. The cleavage planes of the S2 ice were mainly the $\{0\,0\,0\,1\}$ and $\{1\,0\,\bar{1}\,1\}$ planes under the experimental conditions for this study. Kinks forming new grain boundaries were found on the fracture surfaces of polycrystalline S2 ice for the first time. Kinking is regarded as a possible mechanism of plastic deformation for polycrystalline ice and to partially account for the high fracture energy of S2 ice found in this study.

1. Introduction

Early reports on fractographic analyses of ice have been quite brief. While investigating the formation of cracks in ice plates by thermal shock, Gold [1] noted that the fracture surfaces of some straight cracks were very smooth with striated features. The use of the scanning electron microscope (SEM) to examine the fracture surface was first made by Kuroiwa [2]. In a study on the surface topography of etched ice crystals, Kuroiwa paid attention to the features of the fracture surfaces and was able to show well-defined steps or striations on the fracture surface of an ice slab broken by impact. Lavrov [3] visually studied the fracture surfaces of macrocrystalline freshwater (S1) ice from flexure tests and noted conchoidal features in the compression zone and large smooth features in the tension zone. Lavrov made no effort to specify the fracture mechanisms, i.e. cleavage fracture or brittle separation along grain boundaries. Observations on the fracture surfaces of single-crystal ice and columnar-grained polycrystal ice from fracture tests were made by Kusumoto and co-workers [4, 5], who presented a few macrofractographic pictures showing different fracture features corresponding to different testing conditions. More careful fractographic analyses on the fracture surfaces of macrocrystalline S1 ice were carried out by Dempsey and Wei [6]. The latter authors were perhaps the first to attempt to relate the fracture mechanisms to the fracture toughness of freshwater ice. In their study, both cleavage and brittle intergranular fractures were observed in the specimens and associated with different fracture toughness values. There is also a short report by Schulson *et al.* [7], on the observations of fracture surfaces for fine-grained equiaxed freshwater ice ($d \approx 1$ mm) using an environmental scanning electron microscope (ESEM). They found that the fracture mode of this ice type was transgranular cleavage at temperatures around -25 to $-50\,^{\circ}C$.

Nevertheless, compared with the well-developed fractographic techniques for metallic materials, the application of this technique to ice engineering is relatively recent. Our knowledge of the operating fracture mechanisms for various types of ice is still limited. More effort in this direction is needed to fully understand the theoretical and practical problems involving fracture in ice. Recently, the authors of this paper have completed a series of experiments on the fracture of columnar S2 freshwater ice. The fracture mechanisms of the specimens were investigated by combining different techniques: producing a replica of each fracture surface to reveal the fracture features, making thin sections to show the crack path, and using a universal stage [8] to examine the *c*-axis orientations of the cleaved grains as well as the cleavage planes of this ice type.

2. Experimental procedure

Ordinary ice I_h has a hexagonal lattice structure. Each oxygen atom occupying the lattice point is tetrahedrally surrounded by four other oxygen atoms (Fig. 1). As defined by Michel and Ramseier [9], S2 ice is referred to as the ice type with the *c* axes of most grains of the ice sheet being randomly and horizontally or near-horizontally oriented, relative to the surface of the ice sheet. This type of ice has been grown in an insulated tank measuring 1.22 m × 1.14 m × 0.78 m in the cold room at Clarkson University by the following process. The temperature of the cold room was set at $-18\,^{\circ}C$. The tap water in the tank was cooled to about 1 °C at the top surface and 3–4 °C beneath the surface before seeding began. Seeding was performed by spraying a very fine mist upwards above the surface

0022–2461/91 $03.00 + .12

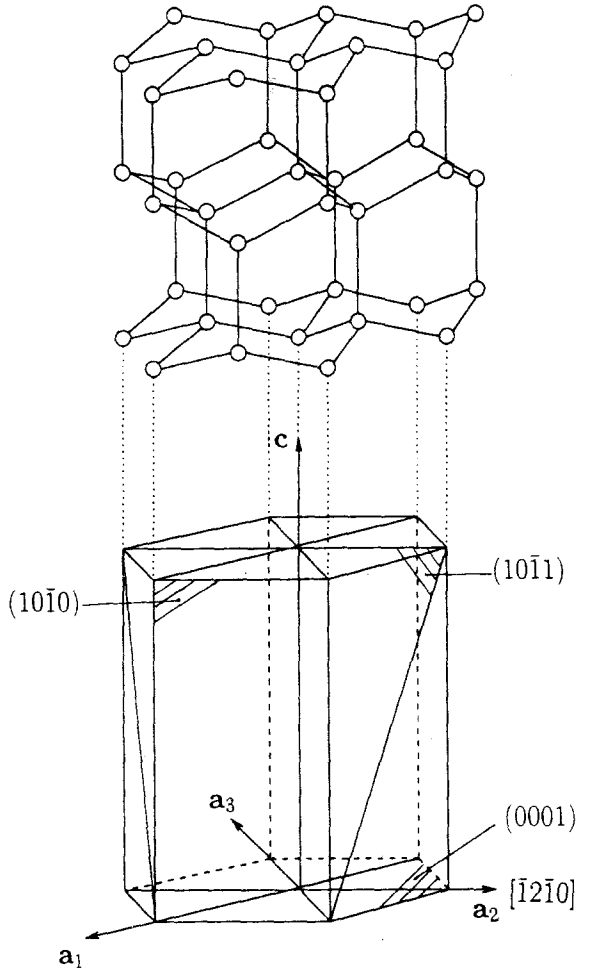

Figure 1 Crystal structure of ice: the open circles are the oxygen atoms, while the hydrogen atoms are not shown. The primitive lattice vectors $\mathbf{a}_1$, $\mathbf{a}_2$, $\mathbf{a}_3$ and $\mathbf{c}$ (the optical or c axis) as well as the basal plane (0 0 0 1), prism plane (1 0 $\bar{1}$ 0) and pyramidal plane (1 0 $\bar{1}$ 1) are shown in the hexagonal cell.

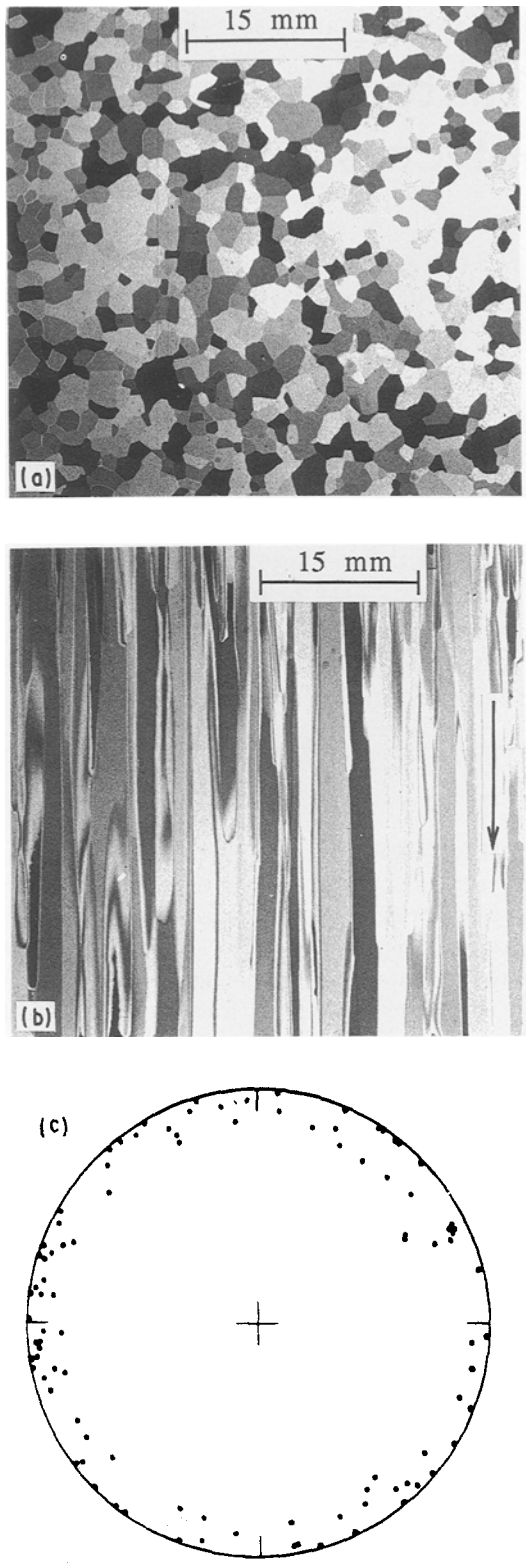

Figure 2 Columnar S2 freshwater ice: (a) horizontal section; (b) vertical section (the arrow indicates the growth direction of the columnar grains); (c) stereographic projection of basal planes of S2 ice measured from the horizontal sections, using a four-axis universal Rigsby stage [8].

of the water. The mist froze to fine ice crystals in the air before reaching the water surface, acting as crystal nuclei to enable the water to solidify heterogeneously. The columnar features of such ice, with the diameter of the columnar grains (typically 2–3.5 mm) increasing with depth, are shown in Fig. 2b. The growth orientation texture of the ice sheet is shown in Fig. 2c which consists of 1 1 0 poles of the basal planes measured by a universal stage from several horizontal thin sections randomly taken from the ice sheet. The conductivity of the meltwater of the specimens tested was $2.40 \pm 0.13 \times 10^{-6}\ \Omega^{-1}\ \mathrm{cm}^{-1}$ at 20 °C and the density was $0.910 \pm 0.003\ \mathrm{Mg\,m^{-3}}$, indicating a low level of impurities and porosity in the ice sheet (compared with the conductivity of $1 \times 10^{-6}\ \Omega^{-1}\ \mathrm{cm}^{-1}$ for distilled water and the bulk density of $0.9187\ \mathrm{Mg\,m^{-3}}$ for ordinary ice at -10 °C [10]).

In this study, fractographic examination was carried out on the fracture surface resulting from Mode I loading conditions. Fracture tests were conducted using both the single-edge notched bend (SENB) and wedge-loaded compact tension (WLCT) loading configurations (Fig. 3), carefully machining specimens cut from the ice sheet. Note that the cracks were vertically oriented so that the plane of the crack was perpendicular to the plane of the ice sheet. In other words, the crack front was parallel to the columnar grains, corresponding to the case of radial cracks found in an ice sheet during the interaction between an ice sheet and a structure. The fracture tests were performed on an ATS universal testing machine at loading rates of $\dot{K} = 10$–$100\ \mathrm{kPa\,m^{1/2}\,s^{-1}}$ so that the specimens were broken within 2–10 s. All tests were done at -10 °C. After the specimens were broken, the fracture surfaces

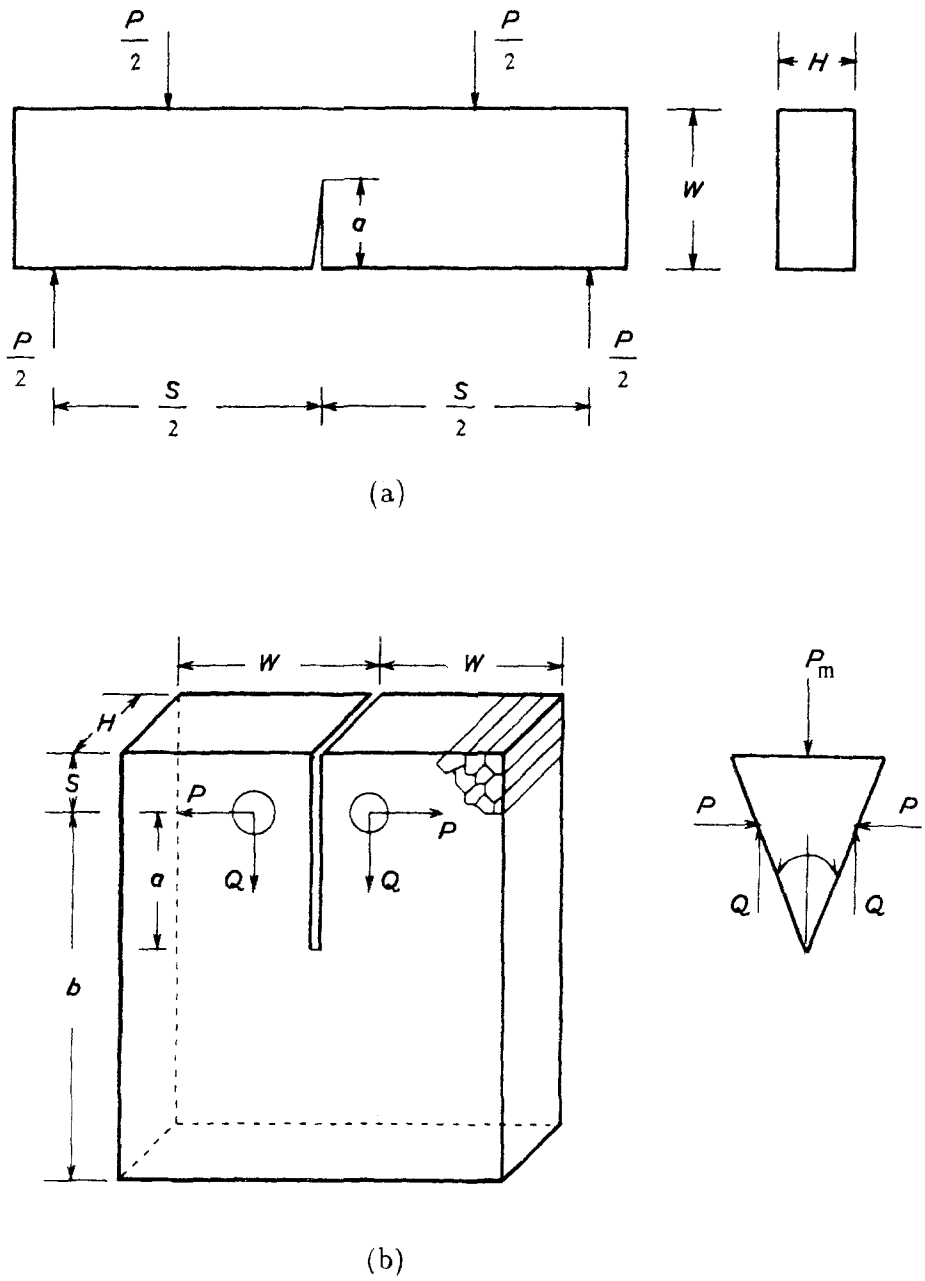

Figure 3 Loading configurations for the fracture tests: (a) SENB and (b) WLCT specimen geometries.

were first examined visually and some fracture characteristics could be detected just by the naked eye. A 6% Formvar solution (6% Formvar in ethylene dichloride) was then dropped on the selected areas of the fracture surface. The solution dried after a period of time and the resulting plastic film replicating the fracture patterns left on the ice surface could be easily peeled off ready for examination. While replicating the fracture patterns, the Formvar solution also etches the fracture surface of the ice specimen, leaving etching pits on the replica. In fact, since being introduced by Schaefer [11], Formvar solutions have previously been used to etch and to duplicate the surfaces of ice crystals in order to reveal slip bands [12] and dislocations [13].

Freshwater ice serves as an excellent material for studies involving the propagation of a crack because of its transparency and large grain sizes. By matching the halves of a broken specimen and making a thin section for the matched specimen, observations of the crack path under polarized light are possible. However, the standard technique of making an ice thin section by melting and refreezing a microtomed ice sample to a glass slide seriously damages the appearance of the crack and makes such observations difficult. In this study, following Daley and Kirby [14], cyanoacrylate glue was used to fix the microtomed samples of the matched specimens to thin-section slides without melting the sample surfaces. The orientation of the thin section with respect to the crack path and microstructure is sketched in Fig. 4. The crack paths of the specimens can be clearly distinguished by this method, as shown in Fig. 5.

When the fracture surfaces of each ice specimen were examined by the naked eye, instances of cleavage failure were clearly evident. For cleavage events, it was necessary to determine the particular cleavage planes relative to each ice crystal. In this study, the technique developed to determine the cleavage planes relied upon measuring the difference of the azimuth angles

between the poles of a fracture plane and the basal plane of the same grain.

3. Fractographic examinations

The grain size of S2 ice is about two or three orders of magnitude larger than that of metals. It is therefore possible to use macrofractography to investigate the fracture mechanisms of the ice specimens. The Formvar replicas of the fracture surfaces were examined by a low-magnification optical lens under inclined lighting. Typical fracture characteristics for the two loading configurations are presented in Fig. 6.

No macro-plastic deformation was detected in these tests, and fracture surfaces were fairly flat. The brittle behaviour of this type of ice was further illustrated by the fact that cleavage and brittle intergranular fracture occurred in both SENB and WLCT specimens. By examining the characteristics of the fracture surface, it was obvious that transgranular fracture was dominant. This observation was confirmed by estimating the proportion of transgranular versus intergranular failure from the thin sections showing crack paths (Fig. 5). From Fig. 5, it is quite clear at a glance that the cracks run transgranularly and intergranularly. The proportion of transgranular versus intergranular failure was approximately determined by counting the numbers of cleaved and intact grains on one side of the crack path. The columnar structure of S2 ice and the fairly flat fracture surface make this approach viable. On average 69% and 74% of grains showed transgranular fracture for the SENB and WLCT specimens, respectively, consistent with observations on the fracture surfaces.

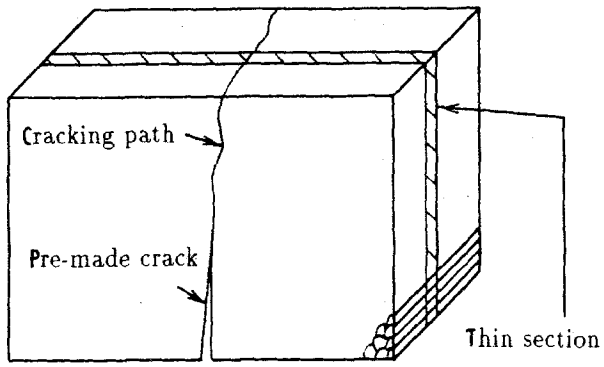

Figure 4 The orientation of the thin section with respect to the crack path.

Fractographic examinations were conducted on the replicas showing fracture patterns (Fig. 6). River patterns are more evident in the grain in the upper part of Fig. 6a (SENB specimen), while the grains below it show purely intergranular failure. A more interesting feature is shown in the middle of Fig. 6b. In a columnar grain, three groups of parallel cleavage steps are mirror-symmetrically oriented with respect to two boundary lines which were probably formed by growth twins during solidification of the ice sheet. In some WLCT specimens, a type of fracture pattern having the characteristics of both cleavage tongue and steps was observed, as shown in Fig. 6d.

A more significant feature in the fracture surfaces of the WLCT specimens is that there are new grain boundaries running generally in the direction of propagation of the crack and across the columnar grains (Fig. 6c and d). The appearance of a new boundary is especially distinguishable in Fig. 6d. These new boundaries were believed to be caused by a "kinking" mechanism. Here, the word kink refers to the

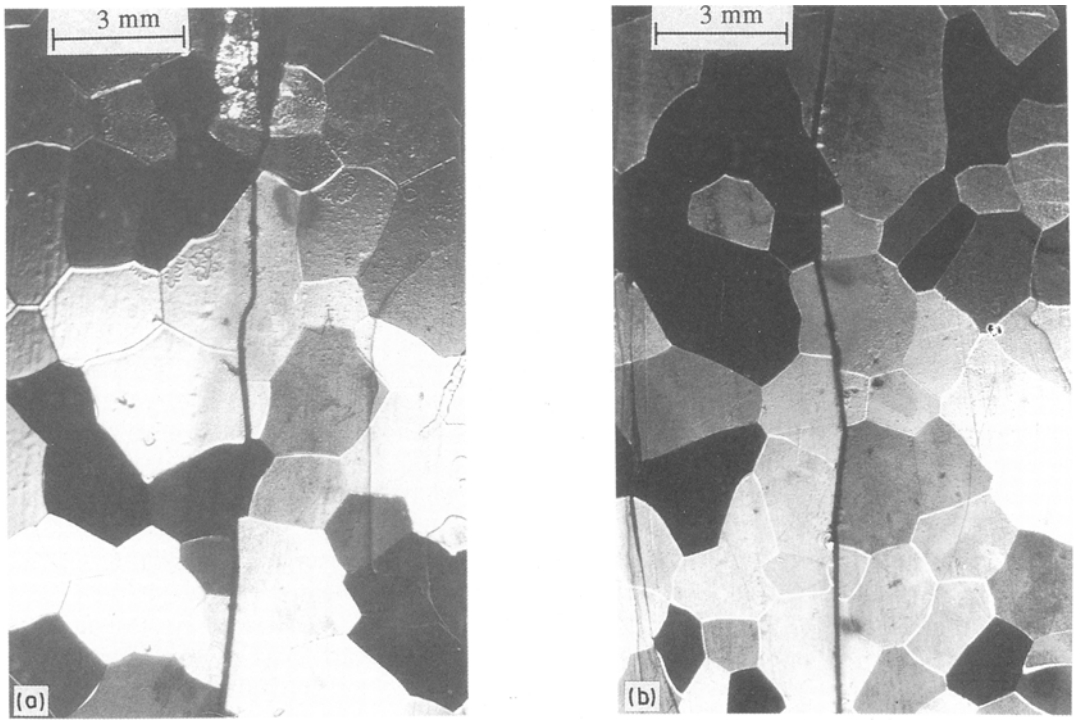

Figure 5 Typical thin sections showing the crack paths and revealing features of transgranular and intergranular fracture (photographed under polarized light): (a) SENB and (b) WLCT fractures.

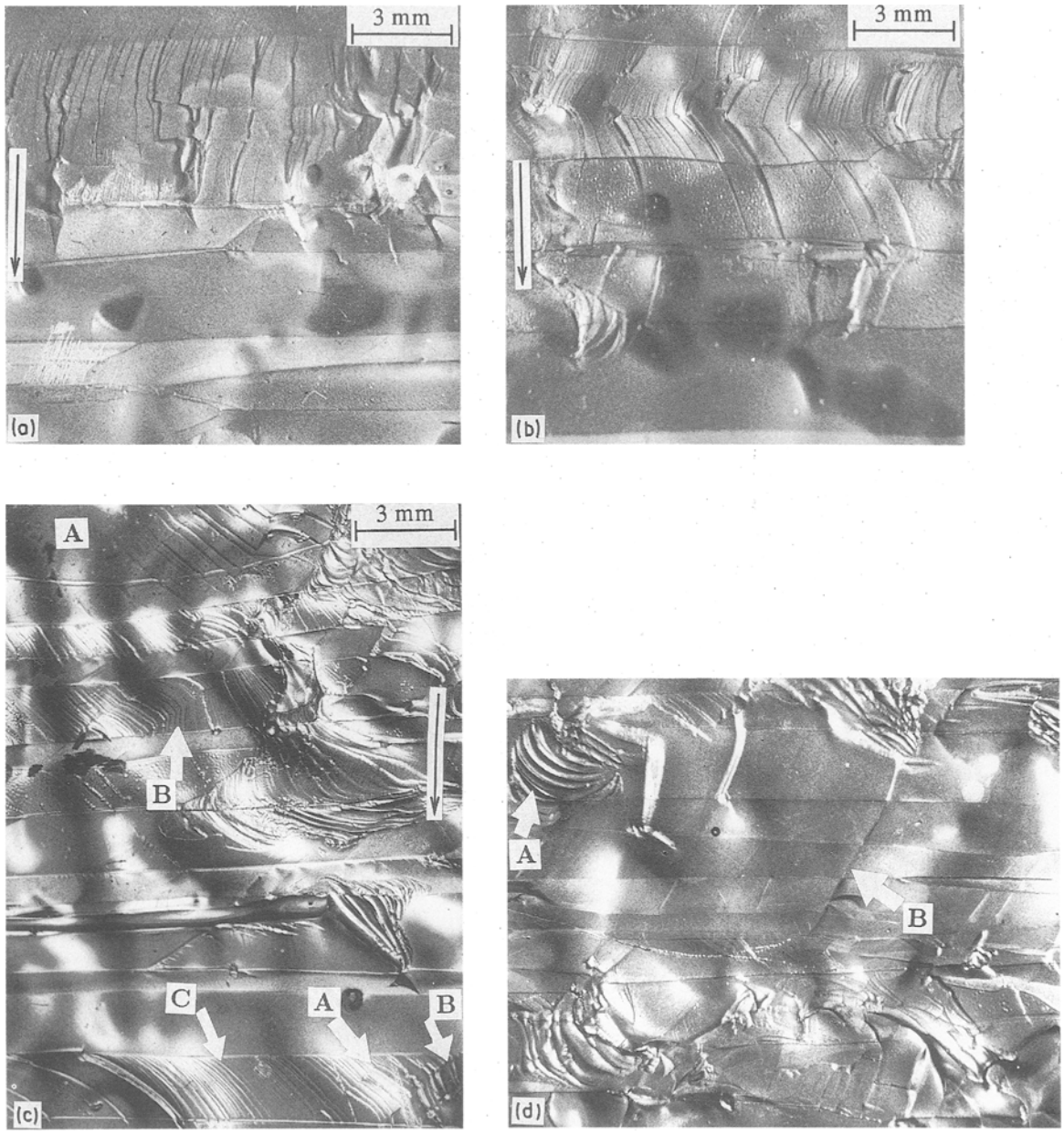

Figure 6 The characteristics of (a, b) SENB and (c, d) WLCT fractures (photographed under inclined lighting); the thin long arrows indicate the directions of propagation of cracks. (a) River patterns and intergranular features; (b) mirror-symmetrically oriented cleavage steps (a lot of etching pits are visible); (c) the interaction between cleavage steps and kinks – the cleavage steps are continuous across the kinks (arrow A), change directions across the kinks (B), or are not disturbed (C); (d) tongue-like steps (arrow A) and kinks (B) across the columnar grains.

deformation mode which was first found by Orowan [15] for metals. In fact, kink bands in mineral crystals were observed a century ago and were sometimes mistaken for twins [16]. It is now known that this type of kinking deformation is common in h.c.p metals such as zinc [15, 16] and magnesium [17]. The kinking deformation in single crystals of ice were reported by Nakaya [18] and Readings and Bartlett [12]. It is important to point out that for h.c.p crystals (either metals or ice), the kinks share essentially the same geometric features in that they are always nearly perpendicular to the basal planes and form non-crystallographic boundaries, although they can be induced by different load conditions such as compression, bending or tension. From Fig. 6c and d it can be argued that the kinks shown are nearly perpendicular to the basal planes if one notes that the basal planes of the columnar grains are parallel or nearly parallel to the growth direction of the columnar grains (see Fig. 2). That is to say, the geometric features of the kinks found for polycrystalline S2 ice in this study are like those found for other materials by previous researchers. Since no kinks were found for the SENB specimens with four-point bend-loading conditions, it is quite possible that the crack-parallel compressive stress component due to the wedge loading and the asymmetrical bending stress induced during loading in the WLCT specimens were responsible for the kinking phenomenon.

While the previous studies on kinking were all conducted on the surfaces of deformed specimens, the observation of kinking for polycrystalline ice in this study was made on the fracture surfaces. This provided an opportunity to investigate the interaction between kinks and topographic patterns of the fracture surface. Fig. 6c clearly reveals the interaction between cleavage steps and kinks or new boundaries. While crossing the kinks some cleavage steps are es-

sentially continuous (location A in Fig. 6c) and some steps change their orientations (location B), although the appearance of the cleavage steps remains the same. Where no new boundary forms, the cleavage steps remain intact (location C). This evidence suggests that these kinks can be regarded as tilt grain boundaries which were formed before the failure of the specimens. The change of orientation of lattice structure across the kinks is fairly small, being consistent with the observations on single ice crystals by Readings and Bartlett [12].

It is necessary to emphasize that the kinks found on the fracture surface indicate the existence of microplastic deformation in polycrystalline S2 ice, even though no macroplastic deformation was detected in this study. This is important since it illustrates that under certain conditions kinking provides a possible mechanism (besides slip) of plastic deformation for polycrystalline ice. It is commonly recognized that the relatively easy basal slip which provides two independent slip systems obviously contributes to the plastic deformation of polycrystalline ice which is of interest to glaciologists. It is not known, however, which of the"hard" planes slip to give the independent slip systems (at least four or five) that are needed for plasticity of hexagonal polycrystals [19]. The prismatic systems $\{1\,0\,\bar{1}\,0\}\ \langle 1\,1\,\bar{2}\,0\rangle$ and the pyramidal systems $\{1\,1\,\bar{2}\,2\}\ \langle\bar{1}\,\bar{1}\,2\,3\rangle$ are possible candidates for making contributions to the plasticity. However, dislocations are rarely observed on the prismatic planes in ice, and dislocations with non-basal Burgers vectors are also rare. Furthermore, non-basal slip is much more difficult than basal slip: the resistance to shear on non-basal planes is at least 60 times greater than that on the basal plane at $-10\,^{\circ}\mathrm{C}$ [20].

The formation of kinks, on the other hand, is relatively easy, and can occur when the resolved shear stress on the slip planes becomes high enough to cause basal plane slip before other modes of deformation intervene [16]. In addition, kinks can be formed over a wide range of loading rates from as fast as the one applied in this study to as slowly as desired [21]. The above considerations reinforce the suggestion that kinking provides a possible mechanism of plasticity for polycrystalline ice.

The fracture energy was found to be $0.6\,\mathrm{J\,m^{-2}}$ for WLCT specimens [22]. For a truly brittle fracture event, the energy needed for a cleavage crack to propagate is equal to twice the surface energy of the material. The surface energy of ice at $-10\,^{\circ}\mathrm{C}$ (the ambient temperature for this study) has not specifically been determined yet. However, while investigating the surface energy of ice crystals, Ketcham and Hobbs [23] suggested that the values of surface energy are not significantly different in the range of temperature between -40 and $0\,^{\circ}\mathrm{C}$. Therefore, the surface energy of ice at $-10\,^{\circ}\mathrm{C}$ is tentatively taken to be $0.1\,\mathrm{J\,m^{-2}}$ which was determined at $0\,^{\circ}\mathrm{C}$ for single crystals [23]. Even taking the effects of temperature on surface energy into consideration (for metals, surface energy increases with decreasing temperature at rates between $0 \sim 3\,\mathrm{mJ\,m^{-2}\,K^{-1}}$), the fracture energy found for WLCT specimens is still appreciably high. It is true that the fracture energy of a polycrystalline material is usually higher than twice the surface energy of the material. However, the kinking phenomenon may well contribute to a higher fracture energy since the formation of kinks dissipates strain energy. For SENB specimens, the apparent fracture toughness K_Q was sought instead of the critical energy release rate. This prevents at this time a comparison of the fracture energies between these two loading configurations. Despite this shortcoming, the effect of the state of stress on the fracture mechanisms of S2 ice is evident.

4. Cleavage planes of S2 ice

As previously mentioned, S2 ice has a very strong growth texture with its c axes horizontally or near-horizontally oriented (Fig. 1). There is also a strong connection between the orientation of the crack and the columnar feature of the ice grains (Figs 2 and 3). In this instance, the basal planes of the columnar grains are parallel or nearly parallel to the crack front, and make certain angles with the fracture plane with two particular orientations being parallel to or perpendicular to the fracture plane. These relations make determination of the cleavage planes for S2 ice possible using a universal stage, as described below.

A thin section showing the crack path was placed on a universal stage. A cleaved grain was chosen and so oriented that the trace of the fracture plane of the grain coincided with the N–S axis, or the A_2 axis of the universal stage. The pole of the fracture plane then falls on the base circle of the stereographic projection and its azimuth angle is 270° as measured on the universal stage. The orientation of the basal plane of the grain is then measured by finding its azimuth angle and inclination angle. The pole of the basal plane is thus decided; 63 fractured grains from five thin sections randomly chosen from the specimens tested were examined in this way. The relative orientation of the cleavage plane with respect to the basal plane of the grain can be determined by finding the difference in azimuth angles of the two poles corresponding to these two planes. In the ideal case, the basal plane is the cleavage plane if the pole of the basal plane coincides with the pole of the fracture plane. If both poles of the basal plane and the fracture plane are on the base circle and differ by 90°, the cleavage plane is then one of the prismatic planes ($\{1\,0\,\bar{1}\,0\}$ or $\{1\,1\,\bar{2}\,0\}$ planes).

In hexagonal systems, the cleavage planes are often found to be the $\{0\,0\,0\,1\}$ or $\{1\,0\,\bar{1}\,1\}$ planes in single crystals [24]. Gold [1] found that the cracks formed in ice crystals by thermal shock were parallel to either basal planes or prismatic planes, indicating that these two groups of crystallographic planes were probably the cleavage planes. It was therefore expected that most poles of the basal planes of the cleaved grains in this study would be randomly distributed around the pole of the fracture planes, or separated by about 90° from it along the base circle.

The results shown in Fig. 7 indicate that the $\{0\,0\,0\,1\}$ planes are indeed the most common cleavage plane.

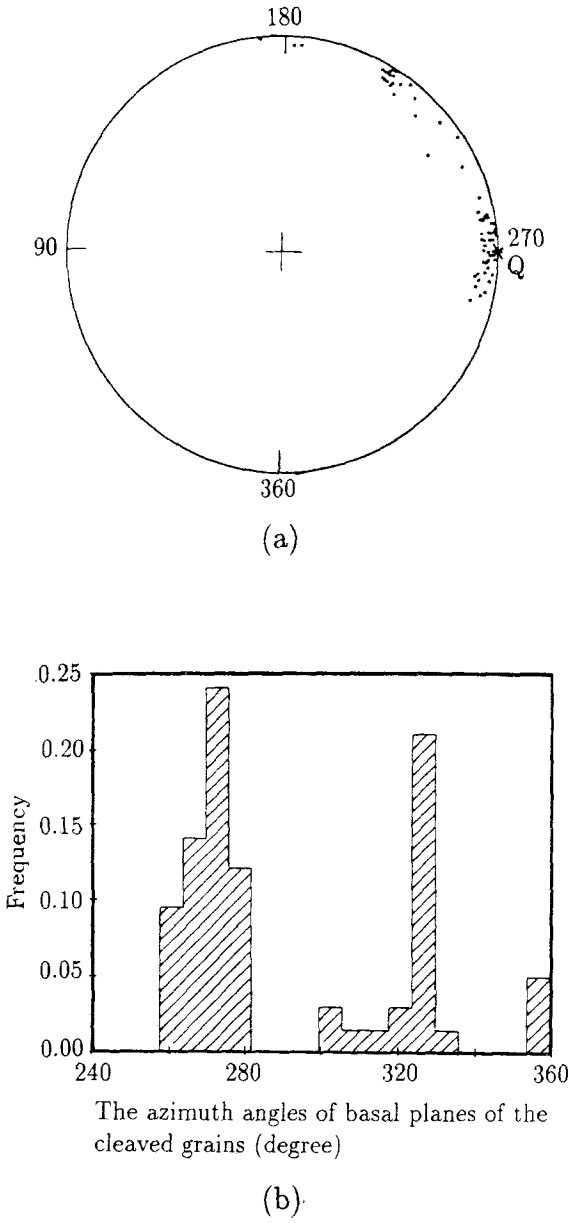

Figure 7 The orientation relations between the basal planes and the fractured planes of cleaved grains: (a) the relative orientations of the basal planes of the cleaved grains with respect to the cleavage planes – note that all the poles of the cleavage planes coincide with point Q (cross mark); (b) the distributions of the relative azimuth angles of the poles of the basal planes of the cleaved grains (the azimuth angles of the cleavage planes are 270° in this figure).

However, only a few poles are about 90° away from the pole of fracture planes. Instead, some poles are concentrated at about 56° from the pole of fracture planes, i.e. measuring 326° on the universal stage. The cleavage planes of these grains from which these poles were found are believed to be the $\{10\bar{1}1\}$ planes which make a crystallographic angle of 62° with basal planes (Fig. 1), the discrepancy in angles resulting from experimental errors. In other words, the $\{10\bar{1}1\}$ planes were the preferred cleavage orientation compared with the $\{10\bar{1}0\}$ planes for S2 ice under the experimental conditions of this study. In fact, the possibility of $\{10\bar{1}1\}$ cleavage had earlier been pointed out by Wakahama [25], who noted that during the cleavage of a laterally compressed single crystal of ice, the fracture path often deviated from the basal planes to non-basal planes which he interpreted as being the prismatic or pyramidal planes. The mechanism of $\{10\bar{1}1\}$ cleavage was investigated by Thornton [26] for single crystals of ζ-Cu–Ge phase; he showed that the formation of $\{10\bar{1}1\}$ twins accompanied by (0001) slip caused cleavage along $\{10\bar{1}1\}$ planes. Whether or not this mechanism actually operates in S2 ice is still unknown. However, the evidence shown in Fig. 7 does suggest the important role of the $\{10\bar{1}1\}$ planes in cleavage fracture of S2 ice.

5. Conclusions

The fracture of S2 ice is a mixture of both cleavage and brittle intergranular fracture. Transgranular fractures were dominant under the conditions for this study. Kinks which formed new grain boundaries were found in polycrystalline ice for the first time, and the importance of kinking in the plastic deformation of polycrystalline ice was emphasized. Under the above experimental conditions, the predominant cleavage planes of S2 ice were the $\{0001\}$ and $\{10\bar{1}1\}$ planes.

Acknowledgements

The assistance of Mr S. J. DeFranco in the experimental work is gratefully acknowledged. This work was supported in part by the US Army under grant DACA 89-86-K-0008, in part by the US National Science Foundation under grant MSM-86-18798, and in part by the US Office of Naval Research under grant N00014-90-J-1360.

References

1. L. W. GOLD, *Canad. J. Phys.* **41** (1963) 1712.
2. D. KUROIWA, *J. Glaciol.* **8** (1969) 475.
3. V. V. LAVROV, "Deformation and Strength of Ice" (translated from Russian) (National Science Foundation, Washington, DC, 1971) p. 37.
4. S. KUSUMOTO, T. TAKASE, T. UCHIDA, T. KIDERA and S. KAJI, *Rep. Fac. Engng Nagasaki Univ.* **15** (1985) 19 (in Japanese).
5. S. KUSUMOTO, N. KIMURA, T. TAKASE and T. KIDERA, *J. Soc. Mater. Sci.* **35** (1986) 887 (in Japanese).
6. J. P. DEMPSEY and Y. WEI, in "Advances in Fracture Research", Vol. 5, ICF7, Houston, 20–24 March 1989, edited by K. Salama, K. Ravi-Chandar, D. M. R. Taplin and P. Rama Rao (Pergamon, Oxford, 1989) p. 3421.
7. E. M. SCHULSON, I. BAKER, C. D. ROBERTSON, R. B. BOLON and R. J. HARNIMON, *J. Mater. Sci. Lett.* **8** (1989) 1193.
8. C. C. LANGWAY Jr, Technical Report No. 62 (US Army Snow Ice and Permafrost Research Establishment, Illinois, 1958).
9. B. MICHEL and R. O. RAMSEIER, *Canad. Geotech. J.* **8** (1971) 35.
10. P. V. HOBBS, "Ice Physics" (Clarendon, Oxford, 1974) p. 348.
11. V. J. SCHAEFER, *Science* **104** (1946) 457.
12. C. J. READINGS and J. T. BARTLETT, *J. Glaciol.* **7** (1968) 479.
13. N. K. SINHA, *Phil. Mag.* **36** (1977) 1385.
14. M. A. DALEY and S. H. KIRBY, *J. Glaciol.* **30** (1984) 248.
15. E. OROWAN, *Nature* **149** (1942) 643.
16. J. J. GILMAN, *Trans. AIME, J. Metals* **200** (1954) 621.
17. A. M. GERVAIS, J. T. NORTON and N. J. GRANT, *ibid.* **197** (1953) 1487.
18. U. NAKAYA, Research Report No. 28 (US Army Snow Ice and Permafrost Research Establishment, Illinois, 1958).

19. J. W. HUTCHINSON, *Met. Trans.* **8A** (1977) 1465.
20. M. F. ASHBY and P. DUVAL, *Cold Regions Sci. Tech.* **11** (1985) 285.
21. J. B. HESS and C. S. BARRETT, *Trans. AIME, J. Metals* **185** (1949) 599.
22. J. P. DEMPSEY, Y. WEI, S. J. DeFRANCO, R. RUBEN and R. FRACHETTI, in "POAC 89", Vol. 1, edited by K. B. E. Axelsson and L. A. Fransson (Lulea, 1989) p. 199.
23. W. M. KETCHAM and P. V. HOBBS, *Phil. Mag.* **19** (1969) 1161.
24. J. J. GILMAN, in "Fracture", edited by B. L. Averbach, D. K. Felbeck, G. T. Hahn and D. A. Thomas (MIT Press, Cambridge, Massachusetts, 1959) p. 193.
25. G. WAKAHAMA, 1965. *Low Temp. Sci. A* **23** (1965) 39 (in Japanese).
26. P. H. THORNTON, *Acta Metall* **13** (1965) 611.

Received 20 April 1990
and accepted 15 January 1991